

## Synthesis of Tetrabenzotriazacorrole–Subphthalocyanine $\mu$ –Oxo Triad

Taniyuki Furuyama, Yusuke Sugiya, and Nagao Kobayashi<sup>@</sup>

Dedicated to Professor Oscar I. Koifman on the occasion of his 70<sup>th</sup> birthday

Department of Chemistry, Graduate School of Science, Tohoku University, Sendai 980-8578, Japan

<sup>@</sup>Corresponding author E-mail: nagaok@m.tohoku.ac.jp

*A  $\mu$ -oxo-linked subphthalocyanine (SubPc)-tetrabenzotriazacorrole (TBC)-SubPc triad has been synthesized. The desired triad could be formed using axial ligand coupling between a TBC phosphorus(V) complex and SubPc, and was characterized by MS, <sup>1</sup>H and <sup>31</sup>P NMR spectra. The triad can absorb light across the entire UV-vis region. Spectroscopic and theoretical analyses support the proposal that the TBC chromophore interacts with the SubPc chromophore.*

**Keywords:** Tetrabenzotriazacorrole, subphthalocyanine,  $\mu$ -oxo-oligomer, absorption spectra.

## Синтез $\mu$ -оксотриады тетрабензотриазакоррола и субфталоцианина

Т. Фуруяма, Ю. Сугия, Н. Кобаяши<sup>@</sup>

Посвящается профессору О. И. Койфману по случаю его 70-летнего юбилея

Химический факультет, Высшая школа наук, Университет Тохоку, Сендай 980-8578, Япония

<sup>@</sup>E-mail: nagaok@m.tohoku.ac.jp

*При взаимодействии субфталоцианина (SubPc) и фосфор(V) тетрабензотриазакоррола (TBC) была получена триада SubPc-TBC-SubPc, связанная  $\mu$ -оксо мостиком через атом фосфора(V). Полученное соединение было охарактеризовано методами масс-спектрометрии и <sup>1</sup>H и <sup>31</sup>P ЯМР спектроскопии. Триада способна поглощать свет в широком диапазоне видимой и УФ области. Спектроскопический и теоретический анализы подтверждают предположение о тесном взаимодействии хромофоров SubPc и TBC.*

**Ключевые слова:** Тетрабензотриазакоррол, субфталоцианин,  $\mu$ -оксо-олигомеры, спектры поглощения.

### Introduction

Tetrabenzotriazacorrole (TBC), the congener of phthalocyanine (Pc), is well known as an 18 $\pi$  electron aromatic macrocycle, in which one *meso* nitrogen atom of Pc is missing.<sup>[1-2]</sup> This molecule retains the tetraisoindole structure, but is a trivalent donor ligand when fully deprotonated. TBCs also have intense absorption bands (the so-called Q and Soret bands) in the UV and visible regions. Tailoring the absorption properties of organic dyes and pigments is one of the most important research topics for

making novel materials, so that a number of Pc derivatives have been designed and synthesized.<sup>[3-4]</sup> Lowering of the molecular symmetry of Pcs plays an important role in tuning the absorption properties; however, the synthesis of these kinds of Pc is often difficult, and yields are low in most cases.<sup>[5-6]</sup> Recently, we proposed a novel strategy for tuning the optical properties rationally using simple synthetic procedures, which is a combination of a simple macrocyclic ligand, peripheral and axial substituents, and main-group elements.<sup>[7-9]</sup> TBCs can be used as an alternative to low-symmetry Pcs in this regard. The direct pyrrole-pyrrole

bond of TBC results in reduced symmetry ( $C_{2v}$ ) compared to regular metalloPcs ( $D_{4h}$ ). TBCs can be accessed by removing the *meso*-nitrogen of the corresponding symmetric Pcs. The yields of TBCs are moderate, while their handling is very easy. Oligomerization of Pcs is also efficient for improving their light-harvesting properties. Taking all of this into consideration, we synthesized and characterized a phosphorus(V) TBC (PTBC)  $\mu$ -oxo homodimer for the first time,<sup>[10]</sup> and demonstrated that the two axial ligands of PTBC are good anchoring groups for the modification of TBCs.

In this paper, we report the synthesis of a TBC-subphthalocyanine (SubPc)  $\mu$ -oxo heterooligomer. SubPcs are  $14\pi$  electron aromatic macrocycles, composed of three 1,3-diiminoisoindole units with a central boron atom.<sup>[11]</sup> SubPcs should have one axial ligand at the boron atom, which can be modified with a functional unit.<sup>[12]</sup> The Q band of typical SubPc appears in the 460-560 nm region, while typical TBC shows little absorption in this region. Therefore, the absorption bands of the  $\mu$ -oxo type heterooligomer may absorb over a wide range of the UV and visible regions, which is a very desirable characteristic for light-harvesting materials. In this paper, the interaction between TBC and SubPc is also discussed, since  $\mu$ -oxo homo and hetero oligomers of Pc derivatives are known to show unique stacking effects.<sup>[13-15]</sup>

## Experimental

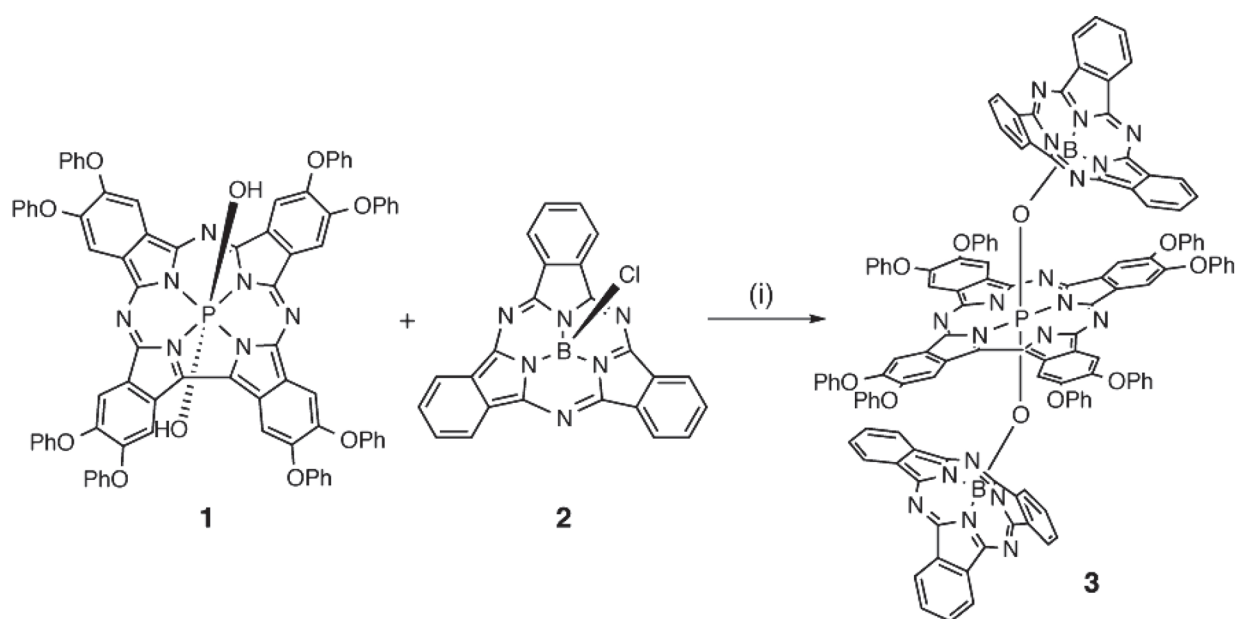
Electronic absorption spectra were recorded on a JASCO V-570 spectrophotometer. NMR spectra were obtained on a Bruker AVANCE III 500 spectrometer. Chemical shifts and coupling constants are expressed in  $\delta$ (ppm) values and in hertz (Hz), respectively.  $^1\text{H-NMR}$  spectra were referenced to the residual solvent as an internal standard.  $^{31}\text{P-NMR}$  spectra were referenced to external 85%  $\text{H}_3\text{PO}_4$  solution (0.0 ppm). The following abbreviations are used: s = singlet, m = multiplet. Mass spectra were recorded on an AB SCIEX 4800Plus TOF/TOF Analyzer.

Compound **1** was synthesized according to a published procedure,<sup>[10]</sup> and compound **2** was purchased from Sigma-Aldrich Inc. and was used without further purification.

**Synthesis of heterotriad (3).** **2** (81.8 mg, 0.19 mmol) and silver triflate (59.1 mg, 0.23 mmol) were dissolved in 1 mL dehydrated toluene, and the mixture was stirred for 1 h. Next, **1** (49.4 mg, 38  $\mu\text{mol}$ ) and *N,N*-diisopropylethylamine (12.3 mg, 95  $\mu\text{mol}$ ) were added to the mixture, and stirred under reflux for 3 h in the dark. After the solvent was removed, the residue was purified by alumina gel chromatography ( $\text{CHCl}_3$ ), followed by size-exclusion chromatography (Bio-Beads S-X1 with  $\text{CHCl}_3$  then toluene). The target compound was obtained as a dark-brownish solid, but the yield could not be determined because the amount was insufficient.  $^1\text{H NMR}$  (500 MHz, toluene- $d_8$ )  $\delta$  ppm: 9.26 (s, 2H), 9.00 (s, 2H), 8.69 (s, 2H), 8.17 (s, 2H), 7.93 (m, 12H), 7.34 (m, 12H), 7.32-7.16 (m, 40H).  $^{31}\text{P NMR}$  (200 MHz, toluene- $d_8$ )  $\delta$  ppm: -212. MS-MALDI ( $m/z$ ) Calcd for  $\text{C}_{128}\text{H}_{73}\text{B}_2\text{N}_{19}\text{O}_{10}\text{P}$   $[\text{M}+\text{H}]^+$ : 2089.6. Found: 2089.5.

## Results and Discussion

The synthetic route for the TBC-SubPc  $\mu$ -oxotriad (**3**) is shown in Scheme 1. TBC with two hydroxyl groups (**1**) was a good precursor of the  $\mu$ -oxo homodimer,<sup>[10]</sup> and the chloride ion at the axial position of SubPc (**2**) can be replaced by alcohols.<sup>[11]</sup> However, direct reaction between **1** and **2** did not proceed, and the desired heterooligomer could not be obtained at all. Torres *et al.* recently reported that an axial ligand of SubPc can be activated by silver triflate. This method utilizes a highly reactive triflate-SubPc intermediate, and, as a result, a wide range of functional groups could be introduced at the axial position of SubPc.<sup>[16]</sup> We applied this method to the reaction with TBC, and finally obtained the desired  $\mu$ -oxo SubPc-TBC-SubPc triad as a dark-brownish solid after separation with size-exclusion chromatography. The solid of **3** was relatively stable under ambient conditions, while **3** decomposed gradually in an oxygen-saturated solution under ambient light.



**Scheme 1.** Synthesis of TBC-SubPc  $\mu$ -oxo triad. Reagents and conditions: (i)  $\text{AgOTf}$ , toluene, rt, 1 h, then  $\text{NEtPr}_2$ , toluene, reflux, 3 h.

The generation of **3** was firstly confirmed by MALDI-TOF-Mass spectroscopy. The observed MS spectrum and calculated isotropic distributions are shown in Figure 1. The strongest peak was found at  $m/z = 2089.5$ , and the isotropic distribution patterns provided a reasonable match with experiment for the compound whose molecular formula is  $C_{128}H_{73}B_2N_{19}O_{10}P$  as a protonated triad ( $[M+H]^+$ ).  $^1H$  and  $^{31}P$  NMR spectra of **1**, **2**, and **3** in pyridine- $d_5$  (**1**) or toluene- $d_8$

(**2** and **3**) are shown in Figure 2. Four sets of singlets (9.6–9.2 ppm) in the  $^1H$  NMR spectrum of **1** are assignable to the  $\beta$ -positions of the TBC macrocycle, reflecting the low-symmetry ( $C_{2v}$ ) structure of the macrocycle. Both the  $^1H$  and  $^{31}P$  NMR spectra of heterotriad **3** exhibit only one set of peaks for the TBC and SubPc units, and each moiety could not be distinguished. The peaks of **3** were observed at higher field than those of **1** and **2**, indicating that each TBC and SubPc moiety is affected by the diatropic ring current generated in the other units, as observed for the TBC  $\mu$ -oxo homodimer.<sup>[10]</sup>

UV-vis absorption spectra of **1-3** in  $CHCl_3$  are shown in Figure 3. The absorption spectra of **1** and **2** show two intense absorption bands. In the case of normal Pcs, the absorption coefficient in the longer wavelength region (the Q band) is larger than for the other band (the Soret band). The absorption envelope of TBC is different from that of Pc, in that the opposite relationship is observed, where the Q band is weaker than the Soret band. The absorption properties of SubPc are similar to those of Pc, but both bands shift to shorter wavelength due to the smaller conjugation system of SubPc. In the spectrum of **1** in the visible region, two intense bands (663 and 450 nm) appear and the absorption coefficients in the 480–600 nm region are negligible. The Q band of SubPc **2** appears at 565 nm, which is midway between the Soret and Q bands of TBC **1**. The absorption spectrum of triad **3** shows three broad absorption bands in the 300–700 nm region. The absorption envelope resembles the sum of that of **1** and **2** in shape, although each band is broadened. Since the absorption peak of the TBC homodimer is broadened due to the electronic interaction of the constituent units, the broad absorption bands of **3** suggest the presence of electronic interactions between the TBC and SubPc units. However, the difference in the positions in the Q band region between **1** and **3** is small (*ca.* 20 nm,  $490\text{ cm}^{-1}$ ) compared with those

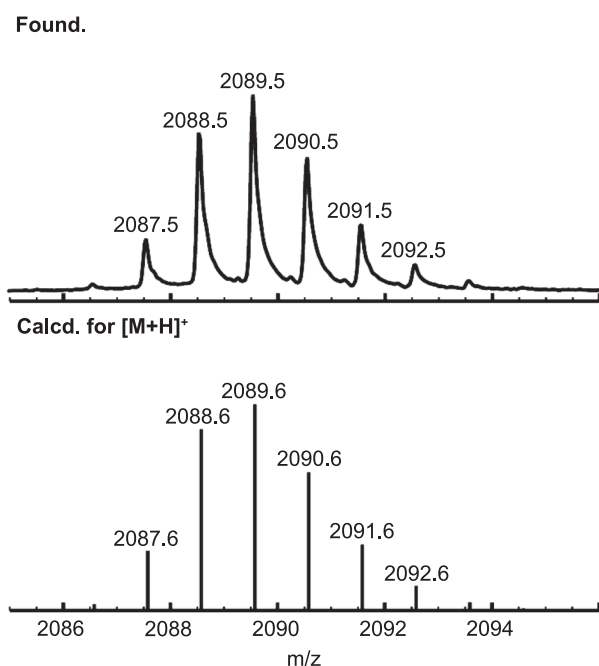


**Figure 1.** MALDI-TOF-MS spectrum of **3** and calculated isotropic distribution pattern for  $C_{128}H_{73}B_2N_{19}O_{10}P$  ( $[M+H]^+$ ).

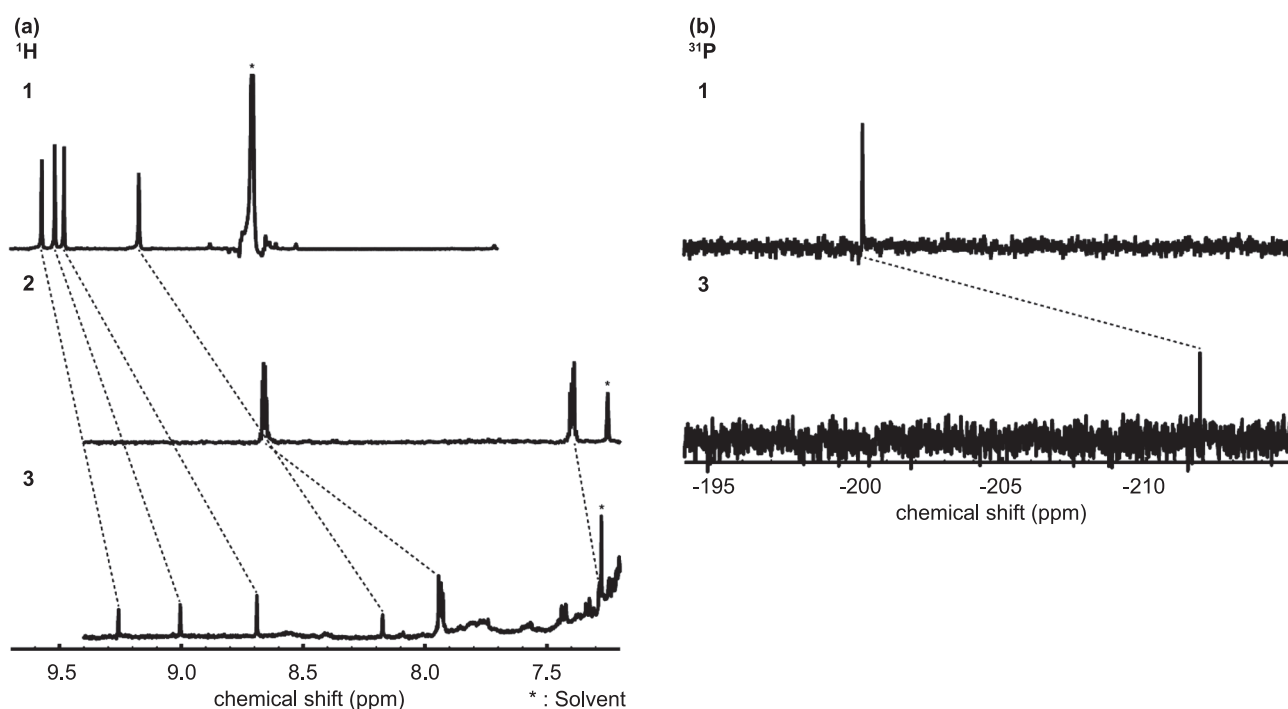


**Figure 2.** (a)  $^1H$  and (b)  $^{31}P$  NMR spectra of **1-3**. Spectra of **1** were recorded in pyridine- $d_5$  solution and the spectra of **2** and **3** were recorded in toluene- $d_8$  solution.

of monomeric TBC and TBC  $\mu$ -oxo dimer (*ca.* 30 nm, 640  $\text{cm}^{-1}$ ),<sup>[10]</sup> since the molecular orbital energies of TBC and SubPc are different.

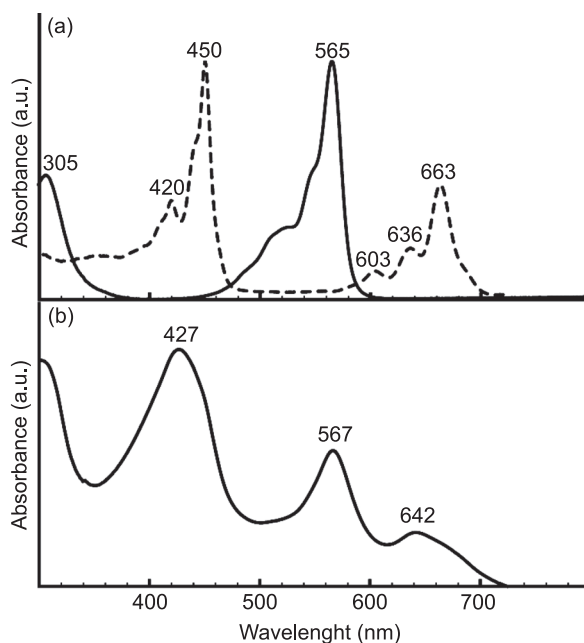


**Figure 3.** UV-vis absorption spectra of (a) **1** (broken lines), **2** (solid lines), and (b) **3** in  $\text{CHCl}_3$ .

In order to estimate the extent of interaction between the TBC and SubPc units of **3**, molecular orbital (MO) calculations were performed for monomeric TBC, SubPc, and TBC-SubPc  $\mu$ -oxo dyad as models of the monomer unit (**1** and **2**) and TBC-SubPc triad (**3**) in this study. Model structure **1'**, in which the substituents on peripheral positions were replaced by hydrogen, was used because these groups only marginally affect the absorption spectra. Model structure **3'** was used as the dyad, while synthesized oligomer **3** was the triad, due to too many atoms of triad for our computational resource. Partial MO energy diagrams of **1'**, **2**, and **3'** are shown in Figure 4, while the calculated absorption spectra of **1'**, **2**, and **3'** are shown in Figure 5, with the calculated transition energies, oscillator strengths (*f*), and configurations summarized in Table 1. The molecular geometries were first optimized at the DFT level using the B3LYP/6-31G(d), as implemented in Gaussian 09.<sup>[17]</sup> The absorption spectra of monomer units **1'** and **2** can be explained by Gouterman's "four-orbital" theory.<sup>[18]</sup> Both the calculated Q (595 and 563 nm) and Soret (399 and 390 nm) bands of **1'** split into two, due to the low-symmetry of the TBC chromophore, and these transitions are composed of the HOMO-1, HOMO, LUMO, and LUMO+1. The calculated Q band (492 nm) of **2** is degenerate, and composed of the HOMO, LUMO, and LUMO+1. The positions of the calculated absorption bands between **1'** and **2** is complementary, and reproduced the

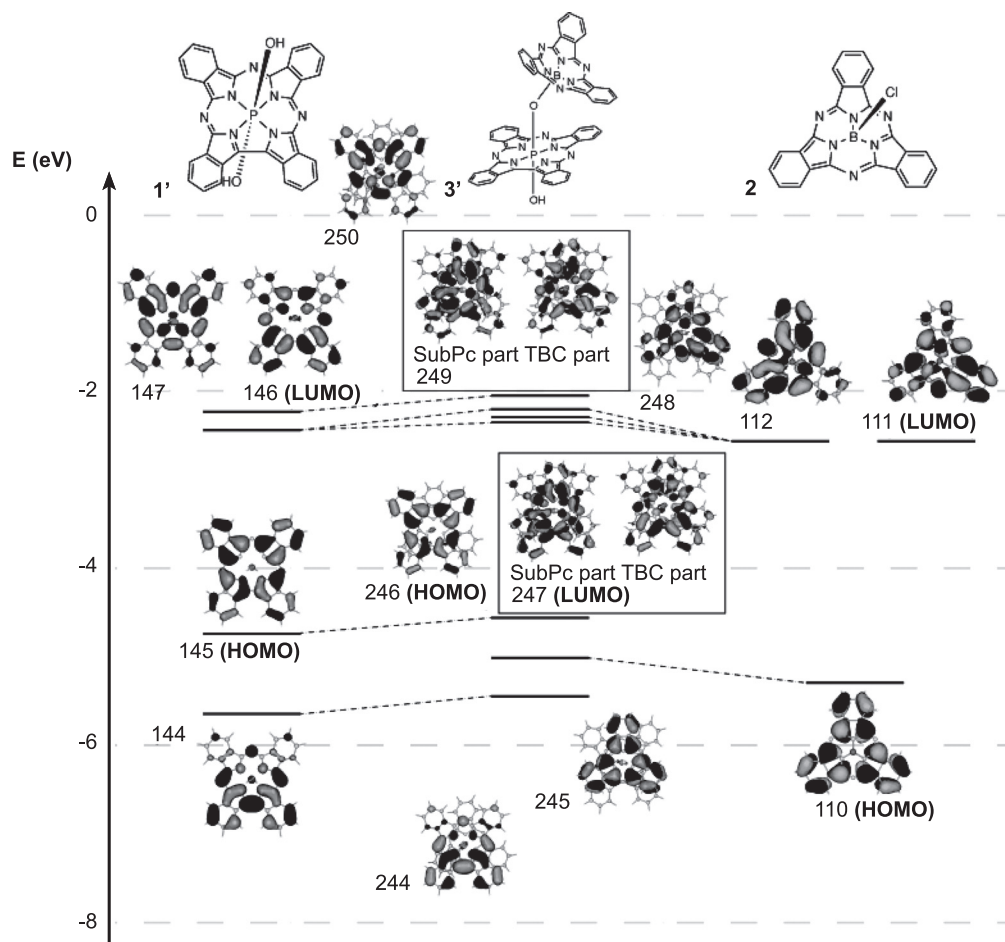


**Figure 4.** Partial molecular energy diagrams and orbitals of TBC (**1'**), SubPc (**2**), and heterodimer (**3'**). Calculations were carried out at the B3LYP/6-31G(d) level of theory.

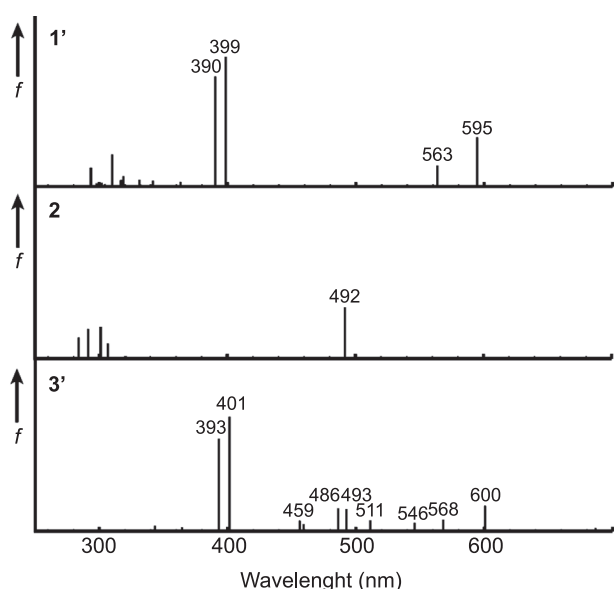


**Figure 5.** Theoretical absorption spectra of **1'**, **2**, and **3'**.

experimental absorption spectra. The calculated absorption spectrum of **3'** is not the sum of **1'** and **2**, estimating many weak transitions over a wide range (ca. 600-400 nm) of the visible region. Although the composition of the transitions of **3'** is more complicated than those of **1'** and **2**, consisting of seven frontier orbitals (from HOMO-2 to LUMO+3), these transitions can be interpreted simply as a linear combination of two almost independent TBC and SubPc chromophores. The HOMO-2, HOMO, and LUMO+3 are localized on the TBC part, while the HOMO-1 and LUMO+1 are localized on the SubPc part. Interestingly, the LUMO and LUMO+2 are delocalized

over the entire complex, and therefore, transitions to these orbitals have an intramolecular charge transfer (CT) character. In addition, as seen from the content of Table 1, all of the relatively intense bands contain CT transitions, but the positions of both the Q and Soret bands are not significantly shifted from those of monomeric TBC and SubPc. The interaction between the TBC and SubPc units appears to be experimentally observed as a broadening of each absorption band.

## Conclusions

A SubPc-TBC-SubPc triad has been synthesized by modification of axial ligands of the central phosphorus(V) ion of the TBC unit. Activation of the axial ligand of SubPc is crucial, and the desired triad **3** was obtained in moderate yield. The observed isotropic distributions in the MS spectrum support the generation of the desired triad, while its NMR spectrum exhibited interaction between the SubPc and TBC units. Moreover, comparison of the absorption spectra among the constituent units and triad also suggests the occurrence of interactions, although the positions of the peaks of the bands were not shifted as much as in the case of a TBC homodimer. [10] Theoretical calculations elucidated the orbital interactions between the SubPc and TBC units. Calculated transitions of the triad model structure are more complicated than the sum of those of SubPc and TBC. Based on the combination of spectroscopic and theoretical results, the stacking effect of the heterooligomer is judged to be weaker than that of the homodimer. The heterooligomer obtained by a simple synthetic procedure can absorb light over the whole UV-visible region, so that it can be a new candidate for functional optical materials, such as photosensitizers in photodynamic therapy or in dye-sensitized solar cells.

**Table 1.** Calculated excited wavelengths ( $\lambda$ ) and oscillator strengths ( $f$ ) for components of selected transition energies.

Compound	$\lambda$ (nm)	$f$	Composition (%) <sup>a</sup>
<b>1'</b>	594.5	0.29	H $\rightarrow$ L (88%), H-1 $\rightarrow$ L+1 (12%)
	563.5	0.12	H $\rightarrow$ L+1 (82%), H-1 $\rightarrow$ L (17%)
	398.6	0.76	H-1 $\rightarrow$ L (80%), H $\rightarrow$ L+1 (17%)
	390.4	0.65	H-1 $\rightarrow$ L+1 (86%), H $\rightarrow$ L (12%)
<b>2</b>	492.0	0.30	H $\rightarrow$ L (95%)
	492.0	0.30	H $\rightarrow$ L+1 (95%)
<b>3'</b>	600.6	0.15	H $\rightarrow$ L+2 (55%), H $\rightarrow$ L (28%), H-2 $\rightarrow$ L+3 (7%)
			H-1 $\rightarrow$ L (6%)
	568.0	0.07	H $\rightarrow$ L+3 (73%), H-2 $\rightarrow$ L (9%), H-1 $\rightarrow$ L (6%)
			H-2 $\rightarrow$ L+2 (3%), H-1 $\rightarrow$ L+2 (3%)
	545.6	0.05	H-1 $\rightarrow$ L (65%), H-1 $\rightarrow$ L+2 (18%), H $\rightarrow$ L+3 (7%)
			H-1 $\rightarrow$ L+2 (3%)
	511.1	0.06	H-1 $\rightarrow$ L+1 (50%), H-1 $\rightarrow$ L+3 (39%), H-1 $\rightarrow$ L+2 (3%)
			H-2 $\rightarrow$ L (3%), H-1 $\rightarrow$ L (2%)
	492.5	0.13	H-1 $\rightarrow$ L+2 (59%), H-1 $\rightarrow$ L+1 (16%), H-1 $\rightarrow$ L (10%)
			H-1 $\rightarrow$ L+3 (5%), H-1 $\rightarrow$ L (5%)
486.1	0.13	H-1 $\rightarrow$ L+3 (51%), H-1 $\rightarrow$ L+1 (22%), H-1 $\rightarrow$ L+2 (11%)	
		H-1 $\rightarrow$ L (7%), H-2 $\rightarrow$ L+1 (5%)	
459.3	0.04	H-2 $\rightarrow$ L+1 (86%), H-2 $\rightarrow$ L+2 (5%), H-2 $\rightarrow$ L+3 (3%)	
		H-1 $\rightarrow$ L+1 (2%)	
401.5	0.67	H-2 $\rightarrow$ L+2 (41%), H-2 $\rightarrow$ L (36%), H $\rightarrow$ L+3 (15%)	
393.2	0.54	H-2 $\rightarrow$ L+3 (83%), H $\rightarrow$ L (5%), H $\rightarrow$ L+2 (5%)	

<sup>a</sup>H-m, H, L, and L+n denote HOMO-m, HOMO, LUMO, and LUMO+n, respectively.

**Acknowledgements.** This work was partly supported by a Grant-in-Aids for Scientific Research on Innovative Areas (25109502, “Stimuli-responsive Chemical Species”), Scientific Research (B) (No. 23350095), Challenging Exploratory Research (No. 25620019) and Young Scientist (B) (No. 24750031) from the Ministry of Education, Culture, Sports, Science, and Technology (MEXT). Some of the calculations were performed using supercomputing resources at the Cyberscience Center of Tohoku University.

## References

- Goldberg D.P. *Acc. Chem. Res.* **2007**, *40*, 626-634.
- Fujiki M., Tabei H., Isa K. *J. Am. Chem. Soc.* **1986**, *108*, 1532-1536.
- Handbook of Porphyrin Science* (Kadish K.M., Smith K.M., Guillard R., Eds.), Singapore: World Scientific Publishing, **2010**.
- The Porphyrin Handbook* (Kadish K.M., Smith K.M., Guillard R., Eds.) San Diego: Academic Press, **2003**.
- Mack J., Kobayashi N. *Chem. Rev.* **2011**, *111*, 281-321.
- Cid J.-J., García-Iglesias M., Yum J.-H., Forneli A., Albero J., Martínez-Ferrero E., Vázquez P., Grätzel M., Nazeeruddin M. K., Palomares E., Torres T. *Chem. Eur. J.* **2009**, *15*, 5130-5137.
- Kobayashi N., Furuyama T., Satoh K. *J. Am. Chem. Soc.* **2011**, *133*, 19642-19645.
- Furuyama T., Satoh K., Kushiya T., Kobayashi N. *J. Am. Chem. Soc.* **2014**, *136*, 765-776.
- Furuyama T., Yoshida T., Hashizume D., Kobayashi N. *Chem. Sci.* DOI: C4SC00569D.
- Furuyama T., Sugiya Y., Kobayashi N. *Chem. Commun.* **2014**, *50*, 4312-4314.
- Claessens C.G., González-Rodríguez D., Rodríguez-Morgade M.S., Medina A., Torres T. *Chem. Rev.* **2014**, *114*, 2192-2277 and references therein.
- Solntsev P.V., Spurgin K.L., Sabin J.R., Heikal A.A., Nemykin V.N. *Inorg. Chem.* **2012**, *51*, 6537-6547.
- Oniwa K., Shimizu S., Shiina Y., Fukuda T., Kobayashi N. *Chem. Commun.* **2013**, *49*, 8341-8343.
- Shimizu S., Matsuda A., Kobayashi N. *Inorg. Chem.* **2009**, *48*, 7885-7890.
- Kleinwächter J., Hanack M. *J. Am. Chem. Soc.* **1997**, *119*, 10684-10695.
- Guilleme J., González-Rodríguez D., Torres T. *Angew. Chem. Int. Ed.* **2011**, *50*, 3506-3509.
- Gaussian 09*, Revision C.01, Frisch M.J., Trucks G.W., Schlegel H.B., Scuseria G.E., Robb M.A., Cheeseman J.R., Scalmani G., Barone V., Mennucci B., Petersson G.A., Nakatsuji H., Caricato M., Li X., Hratchian H.P., Izmaylov A.F., Bloino J., Zheng G., Sonnenberg J.L., Hada M., Ehara M., Toyota K., Fukuda R., Hasegawa J., Ishida M., Nakajima T., Honda Y., Kitao O., Nakai H., Vreven T., Montgomery Jr. J.A., Peralta J.E., Ogliaro F., Bearpark M., Heyd J.J., Brothers E., Kudin K.N., Staroverov V.N., Kobayashi R., Normand J., Raghavachari K., Rendell A., Burant J.C., Iyengar S.S., Tomasi J., Cossi M., Rega N., Millam J.M., Klene M., Knox J.E., Cross J.B., Bakken V., Adamo C., Jaramillo J., Gomperts R., Stratmann R.E., Yazyev O., Austin A.J., Cammi R., Pomelli C., Ochterski J.W., Martin R.L., Morokuma K., Zakrzewski V.G., Voth G.A., Salvador P., Dannenberg J.J., Dapprich S., Daniels A.D., Farkas Ö., Foresman J.B., Ortiz J.V., Cioslowski J., Fox D.J. *Gaussian, Inc.*, Wallingford CT, **2009**.
- Gouterman M. *J. Mol. Spectrosc.* **1961**, *6*, 138.

Received 14.04.2014

Accepted 02.05.2014